

# High voltage capacitors for low background experiments

C. O'Shaughnessy<sup>1,2,a</sup>, E. Andreotti<sup>3</sup>, D. Budjás<sup>4</sup>, A. Caldwell<sup>1</sup>, A. Gangapshev<sup>5,6</sup>, K. Gusev<sup>4,7</sup>, M. Hult<sup>3</sup>,  
A. Lubashevskiy<sup>6</sup>, B. Majorovits<sup>1</sup>, S. Schönert<sup>4</sup>, A. Smolnikov<sup>6</sup>

<sup>1</sup>Max-Planck Institut für Physik, Munich, Germany

<sup>2</sup>Present address: University of North Carolina, Chapel Hill, NC, USA

<sup>3</sup>Institute for Reference Materials and Measurements, Geel, Belgium

<sup>4</sup>Physik Department and Excellence Cluster Universe, Technische Universität München, Garching, Germany

<sup>5</sup>Institute for Nuclear Research of the Russian Academy of Sciences, Moscow, Russia

<sup>6</sup>Max-Planck Institut für Kernphysik, Heidelberg, Germany

<sup>7</sup>Joint Institute for Nuclear Research, Dubna, Russia

Received: 14 March 2013 / Revised: 1 May 2013 / Published online: 25 May 2013

© The Author(s) 2013

**Abstract** Low background experiments place stringent constraints on amount of radioactive impurities in the materials used for their assembly. Often these are in conflict with the constraints placed on the materials by their roles in the experiment. This is especially true for certain electronic components. A high value, high voltage capacitor for use in low background experiments has been developed from specially selected radiopure materials. Electroformed copper foils are separated by polyethylene naphthalate (PEN) foils and supported within a PTFE teflon spiral coil tube. The electrical performance as well as radiopurity are scrutinized here. With some minor modifications to tune the performance for the application, this capacitor can be well suited for a variety of applications in low background experiments. Here the use of the capacitor for high voltage (HV) decoupling in the operation of high purity germanium (HPGe) detectors is demonstrated.

## 1 Introduction

Low-background physics experiments are searching for events with rare signals. The signals are often rarer than typical backgrounds. It is therefore imperative for experiments to be performed in such a manner that the background radiation is kept to a minimum. Some examples of low background physics experiments include: the detection of low energy neutrinos, searches for rare decays (neutrinoless double beta decay, proton decay, e.g.), and direct detection of cold dark matter.

There are a few guiding principles in low background experiments. In addition to defining a unique signal that can be extracted by analysis cuts, one must shield the detectors from any external radiation that may pass the cuts and mimic an event. Some materials, however, must be placed in close proximity to the detectors and cannot be shielded. Therefore, the materials used must be specially selected for radiopurity. A material is considered radiopure when it contains less activity than  $\sim 1$  mBq/kg. While some experience using materials known to be radiopure can go a long way, the selection process typically involves choosing materials that have had minimal processing and then screening the materials for radioactive contaminations [1–3]. If the material is dense and a significant quantity is available, gamma spectroscopy in a low background environment can set limits on the impurity concentrations on the order of  $\mu\text{Bq/kg}$  or less. When less than a kilogram of material is available, direct detection or upper limits on contaminations of the order of parts per billion (ppb) can be placed using Inductively Coupled Plasma-Mass Spectrometry (ICP-MS).

The materials that are in close contact to a low background detector typically have one or more of several functions: mechanical support, electronic support, shielding. Mechanical designs and shielding, while not always straight forward, can be accomplished using a raw material that has had minimal processing and is known to be clean. For the electronic support, conductors and insulators can also be produced from clean raw materials. Electronic components that might perform specialized functions in the signal processing of detectors can pose more challenge. The easiest solution is to move these components outside of the shielding materials, but sometimes this is not possible. Screening for radioactivity may help to select a component that is clean.

<sup>a</sup> e-mail: [chriso@unc.edu](mailto:chriso@unc.edu)

However, it can be difficult to find the appropriate component to meet both technical requirements and radiopurity requirements. This is especially true for discrete components that are highly processed with no regard for radio-purity.

Here we present the design for a simple high voltage (HV) capacitor with a breakdown voltage greater than 5 kV and a capacitance of the order of nano-farads. There are potentially many uses for such a capacitor in low background experiments. For example, this may be used as a filter capacitor in the HV supply line or as a decoupling capacitor to measure the charge collection on a high voltage plane of a detector. In the latter application, additional requirements must be met. The leakage current and micro-discharges must be kept below the noise level of the device being monitored.

The capacitor is produced by layering copper foils with polyethylene naphthalate (PEN) dielectric materials. These layers are rolled and supported using a PTFE spiral coil wrap. The only processing beyond the raw materials is a surface cleaning of the materials and the laser welding of HV cables to the electrode planes. To improve the electrical properties of this capacitor, it is best operated while submerged in a cryogenic liquid. While operation in a high-vacuum environment may in principle also be possible, this option was not pursued and will not be discussed here.

To demonstrate the necessity of this work, a measurement of the radioactivity of a sample of commercially available 1.2 nF NP0 type capacitors was also performed. These capacitors are specified to meet the electrical requirements both at room temperature as well as at liquid nitrogen temperatures. However, it is shown that the radioactivity of these capacitors does not meet the requirements of low background experiments.

The technical specifications and construction of the capacitors will be discussed in detail in Sect. 2.1. Details of the screening measurements performed on the materials selected, the finished capacitors, and the commercial capacitors can be found in Sect. 2.2. Section 3 will address the details of the electrical performance in terms of capacitance, leakage current, long-term stability. Demonstrations of the custom capacitor used to decouple HV from signal in the operation of high purity germanium (HPGe) detectors are presented in Sect. 3.

## 2 Capacitor details

The capacitor presented is an example of a text-book parallel plate capacitor. Prototype capacitors were produced using a principle of minimal processing of screened bulk materials. A screened 25  $\mu\text{m}$  Polyethylene Naphthalate (PEN) film<sup>1</sup> is used for the dielectric material. The conductive surfaces

are a 30  $\mu\text{m}$  oxygen-free electroformed (OFE) grade copper foils.<sup>2</sup> The connections are made through HV cables<sup>3</sup> laser welded directly to the foil. A spiral coil PTFE teflon tube<sup>4</sup> is wrapped around the foils after they have been rolled tightly to support the assembly. The details for the screening results of the individual components are given in Table 1.

### 2.1 Electronic design

The conductive planes are each sandwiched in a PEN foil that is folded over itself. From the two layers of PEN foil, the conductive planes are separated by 50  $\mu\text{m}$ . The relative permittivity for PEN is  $k = 3.0$  [4]. For a 1 nF capacitor, the area of the conducting planes must be approximately 22.5 cm<sup>2</sup>. When operated in liquid nitrogen or liquid argon the relative permittivity, 1.44 and 1.54 respectively [5], will modify this estimate. This effect can be minimized by wrapping the foils tightly to one another. Then the gap between layers is small compared to the PEN foil thickness.

The breakdown voltage of PEN is 300 MV/m [4]. This suggests that the capacitor with 50  $\mu\text{m}$  of PEN separating the conducting planes could be operated with a voltage as high as 15 kV. In a normal laboratory environment there will also be air between the conductive planes that will lower this rating. Dry air at standard temperature and pressure (STP) will breakdown at a minimum voltage of 327 V over a distance of 7.5  $\mu\text{m}$ . This rating will be further reduced by moisture in the air. Due to partial breakdown of gas in the high field

**Table 1** Masses and activities of the bulk materials used in production of the capacitors. In brackets, the mass of materials used in an individual capacitor and the expected contribution of activity is given. The limits are based on a decision threshold calculated at the 90 % confidence level according to Ref. [10]

	<sup>228</sup> Th/ <sup>208</sup> Tl	<sup>238</sup> U/ <sup>214</sup> Bi	<sup>40</sup> K
Teflon Spiral Coil (0.9 g)	<3.3 mBq/kg (<3.0 $\mu\text{Bq}$ )	<2.4 mBq/kg (<2.2 $\mu\text{Bq}$ )	–
PEN Teonex Q51 (0.7 g)	<1.4 mBq/kg (<0.98 $\mu\text{Bq}$ )	<2 mBq/kg (<1.4 $\mu\text{Bq}$ )	<3.6 mBq/kg (<2.5 $\mu\text{Bq}$ )
Cu Foil <sup>a</sup> (1.1 g)	<1.6 mBq/kg (<1.8 $\mu\text{Bq}$ )	<5 mBq/kg (<5.5 $\mu\text{Bq}$ )	<310 mBq/kg (<341 $\mu\text{Bq}$ )
HV Cables (2.2 g)	6 mBq/kg (13.2 $\mu\text{Bq}$ )	<9 mBq/kg (<19.8 $\mu\text{Bq}$ )	58 mBq/kg (127.6 $\mu\text{Bq}$ )
Total (4.9 g)	13.2–19.0 $\mu\text{Bq}$	<28.9 $\mu\text{Bq}$	127.6–471.1 $\mu\text{Bq}$

<sup>a</sup>Results are from ICP-MS measurements of <sup>232</sup>Th and <sup>238</sup>U and therefore rely on an unbroken secular equilibrium of the subsequent decay series

<sup>2</sup>Schlenk Metallfolien GmbH.

<sup>3</sup>Teledyne Reynolds 178-5138.

<sup>4</sup>EAP Elektrotechnische #03-8190020.

<sup>1</sup>Teijin DuPont Films, Teonex Q51.

region, the HV requirement can not be met reliably when operated in gasses at STP.

A typical way to improve a layered device is to include a liquid dielectric that is less reactive than air to displace it from the high field region. The noble liquids exhibit very high resistivity to the ion and electron multiplication that are responsible for the breakdown effects in air. In liquid nitrogen the onset of breakdown starts at 160–190 MV/m and liquid argon at 110–142 MV/m [6]. The capacitors are designed to be operated up to 5 kV with field strengths up to 100 MV/m neglecting fringe field effects. Since this is close to the liquid breakdown, they must be characterized individually for partial breakdown in the desired application.

Since the liquids have a low heat capacity it is believed that bubble formation is the source of discharge events in the liquid cryogenes. References [7, 8] suggest bubble formation may be caused by impurity ions or electrons produced by field emission that are accelerated by the field to create micro-bubble cavitation. If this is the case it may be best to operate the capacitor in a liquid cryogen that is being sub-cooled below the boiling point, as is the liquid argon in the GERDA experiment [9].

## 2.2 Radiopurity

To verify that the radiopurity of all components is suitable for a low background experiment and that the construction process does not introduce further contaminations, gamma spectroscopy measurements have been performed on samples of the materials used to produce the capacitors and listed in Table 1. The gamma screening measurements were performed at the IRMM's Ultra Low-level Gamma-ray Spectrometry (ULGS) facility [11] located in the HADES underground laboratory of the Belgian Nuclear Research Center (SCK-CEN). Due to a low sample mass, ICP-MS measurement of the copper foils was made at the Chemical Service and Chemical Plants of LNGS. The limits placed with ICP-MS are at a 95 % confidence level.

Though an absolute measurement of the activity per each capacitor is limited by the low sample mass, limits are placed on the radiopurity of the significant primordial and anthropogenic isotopes. These values are given in Table 2. The gamma-lines of the most common decay chains could not be identified at a level higher than the backgrounds. However, the secular equilibrium of the uranium series is clearly broken at  $^{210}\text{Pb}$ . It is nevertheless possible that this isotope was introduced through the choice in citric acid for passivation of the copper after etching.

Since the design requires a relatively large surface area, it is prone to contaminations such as  $^{210}\text{Pb}$  and  $^{40}\text{K}$ , that can stick to the surface. As a preventative measure each of the components were etched before construction. This etching removes a layer of the surface and with some efficiency also removes the surface contaminants [12, 13].

**Table 2** Results from gamma screening measurements of eight low background capacitors. Limits for the massic activities as well as absolute limits per capacitor are listed for the primordial  $^{238}\text{U}$  and  $^{232}\text{Th}$  series as well as other radioactive sources.  $^{210}\text{Pb}$  and  $^{40}\text{K}$  could be measured and are discussed in the text. The limits are based on a decision threshold calculated at the 90 % confidence level according to Ref. [10]

	Isotope	Copper-Plane (mBq/kg)	(3.8 g per piece) ( $\mu\text{Bq}$ )
$^{232}\text{Th}$	$^{228}\text{Th}/^{208}\text{Tl}$	<7	<27
Decay Series	$^{228}\text{Ra}$	<11	<42
$^{238}\text{U}$	$^{238}\text{U}$	<40	<153
Decay Series	$^{226}\text{Ra}/^{214}\text{Bi}$	<7	<27
	$^{210}\text{Pb}$	$145 \pm 83$	$555 \pm 317$
	$^{40}\text{K}$	$243 \pm 56$	$930 \pm 215$
	$^{60}\text{Co}$	<4	<15
	$^{137}\text{Cs}$	<3	<12

The etching procedure for the copper follows a recipe designed at Pacific Northwest National Laboratory [13] (The PNNL method). This involves etching the copper in a dilute mixture of sulfuric acid and hydrogen peroxide and then passivating the surface with citric acid to minimize oxidation following the etching step. The polymer surfaces were etched in a solution of nitric acid. While the surface contaminants are removed with some efficiency, there is also the potential for depositing contaminants as well [12]. Care must therefore be taken to use clean chemicals and clean water. The sulfuric (nitric) acid used to etch the materials for the prototype capacitors was an electronic/cleanroom grade specified to have less than 300 ppb (20 ppb) K. The citric acid, on the other hand, did not have a purity specification and could therefore have introduced the contamination that was seen in the measurement. In future productions, more care must be taken in the selection of chemicals used in etching.

A commercial capacitor<sup>5</sup> was also screened to serve as a reference for what cleanliness is available off-the-shelf. The commercial capacitor is a 1.2 nF NPO type capacitor with a maximum operating voltage of 5 kV. The temperature variation is specified to be  $0 \pm 30$  ppm/ $^{\circ}\text{C}$  to a minimum of  $-55$   $^{\circ}\text{C}$ , though this has been shown to hold down to 4 K [14]. Before screening, the 80 capacitors used for the measurement were ultrasonically cleaned in a Tickopur solution and then rinsed in ultrasonic baths of normal and de-ionized water successively. Each ultrasound bath lasted 30 minutes at room temperature and were performed in a flow box that reduced the particle count ( $>0.5$   $\mu\text{m}$ ) of the air to less than 10,000 particles/ $\text{ft}^3$  (cleanroom class 7 [15]).

<sup>5</sup>Novacap #4040N122K502NW.

**Table 3** Results from gamma screening measurements of the Novocap NPO ceramic capacitor. Since the material is proprietary, the activity was calculated for the self shielding of two different possible

material compositions, BaTiO<sub>3</sub> and SiO<sub>2</sub>. The limits are based on a decision threshold calculated at the 90 % confidence level according to Ref. [10]

	Isotope	NPO Commercial Capacitor			
		BaTiO <sub>3</sub> Ni (μBq/g)	(3.0 g per piece) (μBq nom.)	SiO <sub>2</sub> Ni (μBq/g)	(3.0 g per piece) (μBq nom.)
<sup>232</sup> Th Decay Series	<sup>228</sup> Th/ <sup>208</sup> Tl	1120 ± 50	3360	960 ± 40	2880
	<sup>228</sup> Ra	1170 ± 40	3510	1160 ± 40	3480
<sup>238</sup> U Decay Series	<sup>238</sup> U	3010 ± 1400	9030	590 ± 300	1770
	<sup>226</sup> Ra/ <sup>214</sup> Bi	5040 ± 70	15,120	4790 ± 70	14,370
	<sup>210</sup> Pb	9700 ± 3900	29,100	1850 ± 750	5550
	<sup>40</sup> K	3200 ± 200	9600	3300 ± 200	9900
	<sup>60</sup> Co	<13	<39	<13	<39
	<sup>137</sup> Cs	<11	<33	<11	<33

A radioactive decay from within a material is partially shielded by the material itself. In order to calculate the activity of the measured isotope one must know what the material is in order to correct for this effect. Since the ceramic materials of this capacitor are proprietary, we calculate the material dependent detection efficiencies using two ceramics that are commonly used for capacitors [6], BaTiO<sub>3</sub> and SiO<sub>2</sub>. In both of these calculations we also included the Ni contacting surface. The results are shown in Table 3 for both assumptions.

### 3 Electrical tests and performance

Three tests were performed to characterize the capacitors electrically. A precision LCR meter<sup>6</sup> was used to measure the capacitance of the samples both at room temperature and cooled to 77 K in liquid nitrogen. Leakage currents were measured with an electrometer<sup>7</sup> both at room temperature and cooled to 77 K in liquid nitrogen. Application tests were performed to assess suitability as a decoupling capacitor for separating fast signals from a high voltage supply line. A charge sensitive preamplifier<sup>8</sup> was decoupled from the HV cable of a germanium detector operated directly in liquid argon. Two styles of germanium detector were tested: a p-type semicoaxial detector and a Broad Energy Germanium detector (BEGe). Comparisons are made with the case of direct readout from ground in terms of detector resolution and to search for additional events that may come from microdischarges of the capacitors.

<sup>6</sup>Hewlett Packard Model HP4284A.

<sup>7</sup>Keithley Model 6517A.

<sup>8</sup>The preamplifier is a CC2 Model [16] from the GERDA experiment.

#### 3.1 Capacitance measurements

Long term capacitance of the prototypes was measured at low temperatures with HV applied over a period of one week. As the application of a bias voltage is exerting force on the capacitor plates, the bias affects the capacitance. With a stable bias voltage, the capacitance stabilizes over time. Figure 1 shows a set of data that exhibit the longest of these relaxations observed. The capacitor was cooled in liquid nitrogen and biased to 3000 V. After stabilizing and prior to the measurement, the bias was increased to 3500 V. The fit to three exponential decays was performed using a non-linear least squares algorithm. Over the constant value of 1.311 nF the data fit three exponentials with time constants  $439 \pm 10$  sec,  $6753 \pm 37$  sec, and  $89760 \pm 171$  sec and amplitudes of 0.010 nF, 0.015 nF and 0.016 nF respectively. The reduced chi-square of the fit was 1.36.

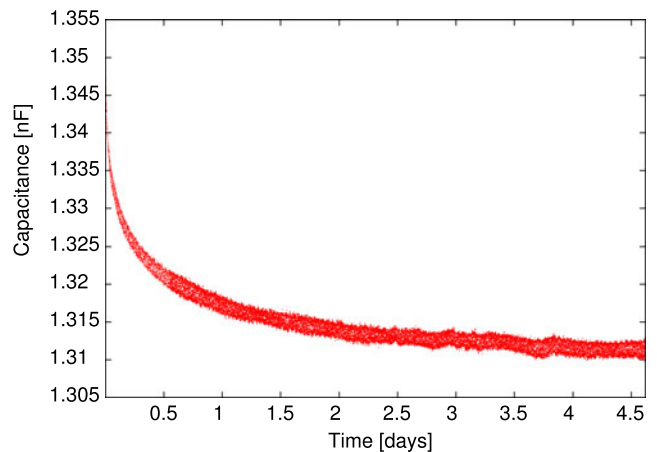


**Fig. 1** Relaxation of the capacitance was observed after applying a bias to the capacitor. The data fit a three component exponential with decay times of roughly 7 minutes, 2 hours, and 25 hours

The use of adhesives or other techniques to bond the layers was excluded to maintain high radio-purity. For this reason the mechanical stability can affect the value of the capacitance. If one assumes that an applied stress will directly affect the capacitance then we can relate the capacitance to the applied stress. It is interesting to note that the change in capacitance associated with applying a bias is greater than the change observed while cooling the capacitor. When the capacitor is cooled from room temperature to 77 K the capacitance is reduced by 80 pF, or 4.5 % over its  $1.82 \pm 0.005$  nF room temperature value. As a bias is applied from 0 V to 5 kV there is also a reduction in the capacitance by 590 pF, or 40 % of its  $1.74 \pm 0.005$  nF value at 77 K with no bias applied. This suggests that the capacitor is strained more by the applied voltage than by the thermal contraction of cooling in liquid nitrogen. There is a linear dependence of the capacitance on the bias voltage, as can be seen in Fig. 2. The reduced chi-square of the linear least squares fit is 2.16.

One possible interpretation of a variation of the capacitance in the measurements could be that due to the ductility of fluoropolymers even at low temperatures, the teflon spiral coil has the ability to expand and contract through a torsional motion. The spiral coil is slowly flexing to accommodate the stress due to a bias voltage or from thermal contractions.

Longterm capacitance was measured with a bias of 5 kV at 77 K and at a sampling rate of 0.3 Hz for a period of five days in order to monitor stability. In these data, shown in Fig. 3, the maximal variation over the measurement period is of 1.2 % and the standard deviation is 0.15 %. The spike structure seen in this figure occurs at regular intervals of once per day within  $\pm 17$  minutes and is assumed to have an environmental origin. Also a cyclic raising and lowering seem to be a temperature dependence in the measurement.

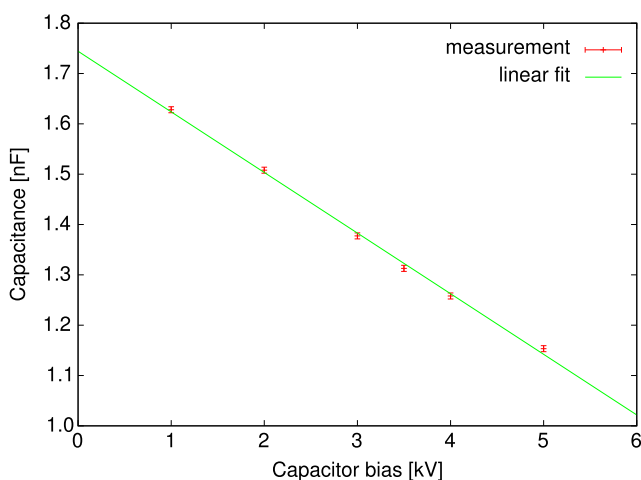


**Fig. 2** Capacitance as a function of the capacitor bias voltage while operated in liquid nitrogen. These values were taken after the capacitor had fully stabilized

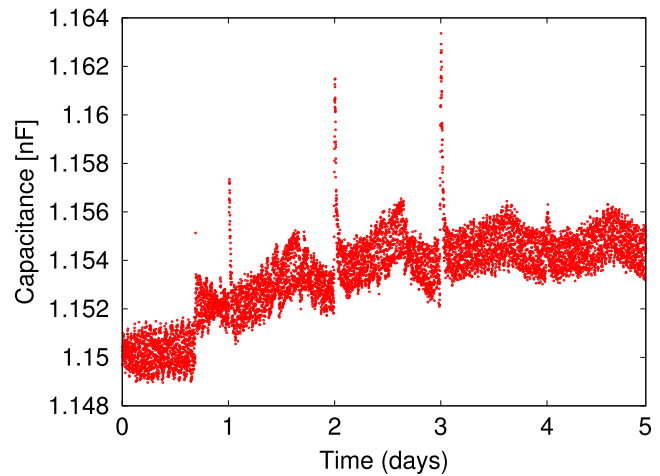


**Fig. 3** Longterm measurement of the capacitance. The capacitor was cooled in liquid nitrogen to 77 K and biased to 5 kV for the duration of this measurement

### 3.2 Leakage current measurements

A good resolution achievable in HPGe detectors is of  $\mathcal{O}(0.77)$  keV or an equivalent noise charge (ENC) of 112 electrons r.m.s [17]. Many of the signal processing parameters, including the signal processing by the preamplifier and the shaping of the signal pulse, contribute to the broadening of the detectors resolution. The leakage current of the capacitor can contribute to the series component of ENC. Typical detectors have a leakage current  $< 10$  pA. This limit must also hold for the leakage current of a decoupling capacitor to maintain the resolution of the detector.

Leakage current at 77 K was measured with the electrometer both at high voltage and without bias. The electrometer was placed in series on the ground end of the capacitor. The capacitor was inside a metal enclosure that was grounded through the shield of the HV supply line to reduce environmental noise. A  $1.0$  G $\Omega$  resistor was placed in-line on the HV side of the capacitor to reduce risk of damaging the electrometer during accidental discharges. At a bias of 5 kV, the mean current measured was 0.67 pA with a Gaussian noise component that had a standard deviation of 1.15 pA. These conditions remained stable over a 7 day measurement period, see Fig. 4. Without a bias, the mean current was at a similar level, 0.59 pA, though the standard deviation of the measurement was significantly smaller, 0.003 pA.

### 3.3 Detector application tests

Standard HPGe detectors with only two contacts are typically operated with HV on the larger outer contact and the signal read from a smaller inner contact directly with the virtual ground through the preamplifier. The smaller contact

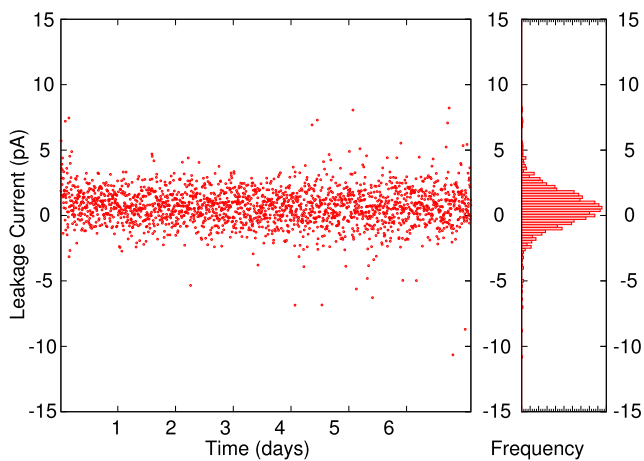


**Fig. 4** Long-term measurement of the leakage current with the capacitor biased to 5 kV at 77 K. The right hand projection is a binned frequency distribution showing the Gaussian profile

typically has a smaller stray capacitance to pick up environmental noise. Consequently, a higher resolution is achievable by monitoring this contact. In this bias configuration the contact is directly coupled to the preamplifier and is therefore referred to as a DC coupled readout. In principle one could reverse the bias and exchange the contacts to achieve the same electric field in the detector, though then the resolution is typically degraded when reading the larger contact. However, if one decouples the HV from the preamplifier using a high valued capacitor, the fast signal pulse can pass through the decoupling capacitor to the preamplifier. This so-called AC coupled readout maintains the higher resolution of the readout from the core contact. Figure 5 shows a diagram of a semi-coaxial detector. This shows how the

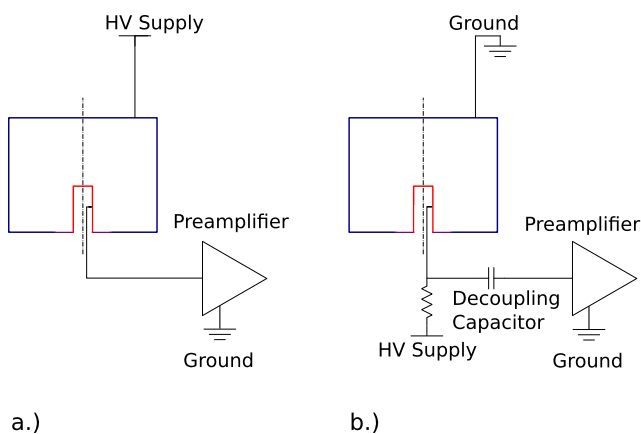


**Fig. 5** This diagram represents the two readout schemes: (a) DC readout and (b) AC readout. Here the semi-coaxial detector is shown in cross section with its axis of rotational symmetry displayed by the dashed centerline. The outer surface is shown in blue, and the inner contact is shown in red. The AC readout requires two additional clean components. A decoupling capacitor as well as a resistor in the HV line impeding the signal through that channel

inner contact is better shielded from stray capacitance and highlights the DC and AC readout configurations.

The main goal of this work is to develop a low radioactivity capacitor used as a decoupling capacitor in the AC operation of a germanium detector. To quantify the suitability of this capacitor, a semi-coaxial prototype detector for the GERDA experiment was operated in the AC configuration with both the detector and the capacitor submersed directly in the liquid argon coolant in the Gerda Detector Laboratory (GDL) testbench. Spectroscopic measurements of a  $^{60}\text{Co}$  source provide a reference for the resolving power of the 1.3 MeV  $\gamma$ -line emitted in this decay. The best resolution of this peak for the detector DC coupled in the same cryostat used here was 2.5 keV FWHM. Here we have achieved a resolution of 2.6 keV FWHM with the detector AC coupled through the capacitor. A BEGe detector that normally had a resolution of 1.8 keV at the 1.3 MeV  $\gamma$ -line was also operated in the same test stand in AC mode. In this configuration the detector had a resolution of 1.9 keV.

### 3.4 Microdischarge tests

One concern when a detector is operated in AC mode is that microdischarges of the capacitor can cause signal like events in the energy region of interest. For example, a signal of 1 MeV in a germanium detector is identified by the collection of the charge of  $\sim 335,000$  electrons, or  $\sim 54$  fC. If a capacitor of 1.0 nF is biased with a germanium detector to 4 kV the charge stored is  $\sim 4$   $\mu\text{C}$ . Therefore a fractional discharge of even  $10^{-7}$  of the total charge stored leads to background in the detector.

The information here is inferred from detectors operated in the AC configuration, where the events can be generated from energy deposits in the germanium, or from microdischarge pulses from the capacitor or HV cables. Tests were performed using a BEGe detector operated in AC mode in the LARGE [18, 19] test facility. The main purpose of these tests was to study the reduction in  $^{42}\text{K}^+$  collected on the surface of the detector operated in AC mode. The liquid argon in this facility has been doped in the ion's parent isotope  $^{42}\text{Ar}$  to enhance the effect.

In searching for the effect of discharges in the capacitor only the higher energy events are used where the actual energy deposit in HPGe detectors is expected to be rare. For example, the beta decay of  $^{42}\text{K}$  has an endpoint energy of 3.5 MeV. In Table 4, the event rate for  $>4.4$  MeV is given for each of the measurements. The measurement of a detector in the DC configuration confirms the low rate of events above this threshold. Measurement of the same detector in AC configuration using a capacitor of the original design was performed without the use of a buffer resistor in the HV line. Therefore, in addition to a high count rate above the energy threshold, this measurement also displayed a low

**Table 4** The event rate above an energy threshold of typical expected background decays in HPGe detectors used as an indicator for potential microdischarge events in the capacitor. DC configured detectors are without the decoupling capacitor to compare with expected rates above this threshold

Detector	Configuration	Bias voltage	Rate >4.4 MeV (cts/kg-day)
BEGe	DC mode in LARGE	4.0 kV	0.19 (90 % CL)
BEGe	AC mode in LARGE	4.0 kV	94(4)
BEGe	AC mode in LARGE with 3-Layer Capacitor <sup>a</sup>	4.0 kV	0.65

<sup>a</sup>An additional PEN layer was added to the capacitor giving the foils a separation distance of 75  $\mu\text{m}$  and reducing the capacitance to 0.8 nF (nom.)

resolution. A second measurement of the AC configuration was performed with the addition of a 300 M $\Omega$  resistor in the HV line, Fig. 5b, as well as a new decoupling capacitor with a third layer of PEN separating the capacitor planes. Increasing the separation of the copper planes reduces the electric field in the capacitor and as a result is expected to reduce the rate of microdischarges.

#### 4 Recommendations and conclusions

In the course of these studies it was seen that the performance of capacitors of this construction can be tailored to the application. With supporting screening measurements, a polyvinyl fluoride shrink tube could provide higher mechanical and electrical stability than the PTFE spiral coil tube. In higher voltage applications the thickness of the PEN foil could be increased to improve the resistivity to microdischarges. If one does not need the high voltage specified, the thickness of the foil could also be reduced to minimize the material usage, thereby minimizing radioactivity. If the application is sensitive to microdischarges, additional cleaning procedures to scrub the dielectric surfaces could help to reduce surface currents. Additionally, a floating copper foil could be placed in the center of the capacitor to help reduce field strength especially at the edges of the capacitor planes.

A low background, high value, and high voltage capacitor for operation in a cryogenic liquid has been developed and characterized. With a value of  $\sim 1.5$  nF, a breakdown voltage greater than 5 kV, and a leakage current less than 10 pA, the performance meets the specified requirements and is acceptable for the applications of HV decoupling or as a HV filter capacitor. In the operation of low background HPGe detectors one must also be careful about microdischarges that can

cause signal-like events. Here we have shown that increasing the separation distance of the electric planes, thereby reducing the field strength, helps to mitigate this effect.

**Acknowledgements** The authors would like to thank Stefano Nisi for his technical support of the ICP-MS measurements as well as Bernhard Schwingenheuer for his critical review of the work.

#### References

1. G. Heusser, *Annu. Rev. Nucl. Part. Sci.* **45**, 543 (1995)
2. H. Neder, G. Heusser, M. Laubenstein, *Appl. Radiat. Isot.* **53**, 191 (2000)
3. J.A. Formaggio, C. Martoff, *Annu. Rev. Nucl. Part. Sci.* **54**, 361 (2004)
4. Teijin Dupont Films, *Technical Data: Teonex Q51*. URL <http://www.tejindupontfilms.jp/english/product/msds/index.html>
5. D.R. Johnston, G.J. Oudemans, R.H. Cole, *J. Chem. Phys.* **33**(5), 1310 (1960)
6. M. Naidu, V. Kamaraju, *High Voltage Engineering*, 4th edn. (McGraw-Hill, New Delhi, 2009), p. 79
7. D. Peier, *J. Electrostat.* **7**(0), 113 (1979)
8. J. Gerhold, *Cryogenics* **38**(11), 1063 (1998)
9. K.H. Ackermann et al., *Eur. Phys. J. C* **73**, 1 (2013)
10. ISO 11929-3. Determination of the Detection Limit and Decision Threshold for Ionizing Radiation Measurements. International Organization for Standardization, Geneva, Switzerland (2000)
11. E. Andreotti, M. Hult, R.G. de Orduña, G. Marissens, M. Mihailescu, U. Wätjen, P.V. Marcke, in *The 3-rd International Conference Current Problems in Nuclear Physics and Atomic Energy*, vol. Part 2 (Publishing Department of KINR, 2011), vol. Part 2, pp. 601–605
12. G. Zuzel, M. Wójcik, B. Majorovits, M. Lampert, P. Wendling, *Nucl. Instrum. Methods Phys. Res., Sect. A, Accel. Spectrom. Detect. Assoc. Equip.* **676**(0), 149 (2012)
13. E. Hoppe, A. Seifert, C. Aalseth, P. Bachelor, A. Day, D. Edwards, T. Hossbach, K. Litke, J. McIntyre, H. Miley, S. Schulte, J. Smart, G. Warren, *Nucl. Instrum. Methods Phys. Res., Sect. A, Accel. Spectrom. Detect. Assoc. Equip.* **579**(1), 486 (2007)
14. F. Teyssandier, D. Prêle, in *Ninth International Workshop on Low Temperature Electronics—WOLTE9*, Guarujá, Brazil (2010)
15. ISO/DIS 14644-1. Classification of Air Cleanliness. Institute of Environmental Sciences and Technology, Arlington Heights (IL), USA (2010)
16. S. Riboldi, C. Cattadori, A. D'Andragora, A. Pullia, F. Zocca, M. Barnabé-Heider, D. Budjas, in *Nuclear Science Symposium Conference Record (NSS/MIC), 2010 IEEE* (2010), pp. 1386–1388
17. A. Pullia, F. Zocca, S. Riboldi, *IEEE Trans. Nucl. Sci.* **55**(1), 591 (2008)
18. M. Heisel, Large—a liquid argon scintillation veto for gerda. Ph.D. thesis, Universität Heidelberg (2011). URL <http://www.ub.uni-heidelberg.de/archiv/11921>
19. M. Agostini, M. Barnabé-Heider, D. Budjáš, C. Cattadori, A. D'Andragora, A. Gangapshev, K. Gusev, M. Heisel, M. Junker, A. Klimenko, S. Schönert, A. Smolnikov, G. Zuzel, *J. Phys. Conf. Ser.* **375**(4), 042009 (2012)